Article
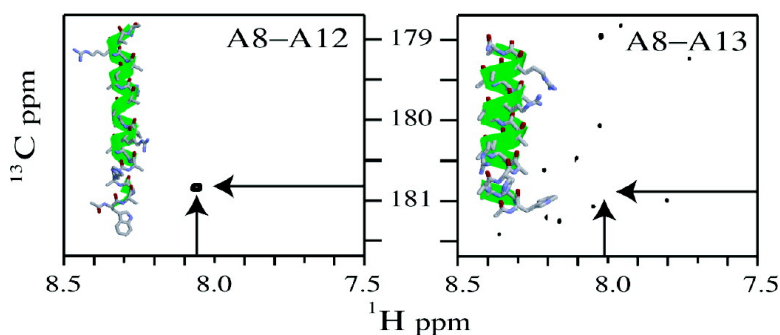
Discriminating the Helical Forms of Peptides by NMR and Molecular Dynamics Simulation

Darn I. Freedberg, Richard M. Venable, Angelo Rossi, Thomas E. Bull, and Richard W. Pastor

More About This Article

Additional resources and features associated with this article are available within the HTML version:

- Supporting Information
- Links to the 2 articles that cite this article, as of the time of this article download
- Access to high resolution figures
- Links to articles and content related to this article
- Copyright permission to reproduce figures and/or text from this article

View the Full Text HTML

Discriminating the Helical Forms of Peptides by NMR and Molecular Dynamics Simulation

Darón I. Freedberg, Richard M. Venable, Angelo Rossi,[†] Thomas E. Bull, and
Richard W. Pastor*

*Contribution from the Laboratory of Biophysics, Center for Biologics Evaluation and Research,
Food and Drug Administration, 1401 Rockville Pike, Rockville, Maryland 20852*

Received March 19, 2004; E-mail: pastor@cber.fda.gov

Abstract: The HNCO NMR pulse sequence was applied to three selectively labeled ^{15}N and ^{13}C isotopic homologues of the peptide Ac-WAAAH(AAARA)$_3$A-NH$_2$ to probe directly for hydrogen bonds between residues 8 and 11 (characteristic of a 3_{10}-helix), 8 and 12 (α-helix), and 8 and 13 (π-helix). The experiments demonstrate conclusively, and in agreement with circular dichroism studies, that the center of the peptide is α-helical; there is no discernible 3_{10}- or π-helix at these specific positions. Molecular dynamics simulations of the preceding peptide and Ac-(AAAAK)$_3$A-NH$_2$ in water using the potential energy parameter set CHARMM22/CMAP correctly yield an α-helix, in contrast to simulations with the set CHARMM22, which result in a π-helix.

Introduction

The primary helical forms in proteins, 3_{10}, α, and π, are distinguished by hydrogen bonds between residues i and $i + 3$, $i + 4$, and $i + 5$, respectively. Even though the α-helix is common and the π-helix is rare in proteins,[1] a number of recent molecular dynamics (MD) simulations of peptides presumed to be α-helical have yielded significant populations of π-helix.[2−12] As an example, Figure 1 shows the fraction of α- and π-helix from simulations of two different peptides[13,14] with the CHARMM[15] parameter set C22.[16] In each case, the peptide converted from α- to π-helical within 5 ns. Motivated by these and previously published results, Feig, MacKerell, and Brooks[17] carried out high-level ab initio calculations of the ϕ ($C-N-C_\alpha-C$),ψ ($N-C_\alpha-C-N$) surface of the model dipeptide N-acetylalanyl-N'-methylalaminde (AAMA), and they determined that the energy of the π-helical conformation is 2.6 kcal/mol higher than that of the α-helical conformation. In contrast, the energies of these conformations of AAMA in a vacuum are equal for C22. (Differences for other major force fields are included in Table 1 of ref 17.) While this information does not necessarily indicate which conformation of a longer peptide will be stable in water, the stability of π-helices in simulations using C22 is not surprising.

MacKerell et al.[18] then developed a new potential that employs a grid correction to the C22 ϕ,ψ surface to match the ab initio surface. The grid correction was adjusted slightly to reproduce crystal structures of a variety of proteins. Simulations of AAMA in water[18] and of (AAQAA)$_3$ with implicit solvent[17] based on this potential successfully produced α-helical conformations. A recent revised version of the potential[19] includes improvements to the proline and capping residues and will henceforth be denoted C22/CMAP, where CMAP stands for "cross-term map".

This article first answers the question: Will C22/CMAP yield the α-helical conformations for Ac-WAAAH(AAARA)$_3$A-NH$_2$ (here denoted *Hlx*) and Ac-(AAAAK)$_3$A-NH$_2$ (denoted 3K(I)) in water? This is addressed because validation of the potential

† IBM Research Division, T. J. Watson Research Center, Yorktown Heights, NY 10598.

(1) Creighton, T. E. *Proteins: Structures and Molecular Properties*; W. H. Freeman: New York, 1993.
(2) Kovacs, H.; Mark, A. E.; Johansson, J.; van Gunsteren, W. F. *J. Mol. Biol.* **1995**, *247*, 808−822.
(3) Shirley, W. A.; Brooks, C. L., III. *Proteins* **1997**, *28*, 59−71.
(4) Sessions, R. B.; Gibbs, N.; Dempsey, C. E. *Biophys. J.* **1998**, *74*, 138−152.
(5) Duneau, J.-P.; Crouzy, S.; Chapron, Y.; Genest, M. *Theor. Chem. Acc.* **1999**, *101*, 87−91.
(6) Dominy, B. N.; Brooks, C. L., III. *J. Phys. Chem. B* **1999**, *103*, 3765−3773.
(7) Pak, Y.; Wang, S. *J. Chem. Phys.* **1999**, *111*, 4359−4361.
(8) Lee, K.-H.; Benson, D. R.; Kuczera, K. *Biochemistry* **2000**, *39*, 13737−13747.
(9) Hiltpold, A.; Ferrara, P.; Gsponer, J.; Caflish, A. *J. Phys. Chem. B* **2000**, *104*, 10080−10086.
(10) Pak, Y.; Jang, S.; Shin, S. *J. Chem. Phys.* **2002**, *116*, 6831−6835.
(11) Kohtani, M.; Jarrold, M. F. *J. Am. Chem. Soc.* **2002**, *124*, 11148−11158.
(12) Armen, R.; Alonso, D. O. V.; Daggett, V. *Protein Sci.* **2003**, *12*, 1145−1157.
(13) Thompson, P. A.; Eaton, W. A.; Hofrichter. J. *Biochemistry* **1997**, *36*, 9200−9210.
(14) Marqusee, S.; Robbins V. H.; Baldwin, R. L. *Proc. Natl. Acad. Sci. U.S.A.* **1989**, *86*, 5286−5290.
(15) Brooks, B. R.; Bruccoleri, R. E.; Olafson, B. D.; States, D. J.; Swaminathan, S.; Karplus, M. *J. Comput. Chem.* **1983**, *4*, 187−217.

(16) MacKerell, A. D., Jr.; Bashford, D.; Bellott, M.; Dunbrack, R. L., Jr.; Evanseck, J.; Field, M. J.; Fischer, S.; Gao, J.; Guo, H.; Ha, S.; Joseph, D.; Kuchnir, L.; Kuczera, K.; Lau, F. T. K.; Mattos, C.; Michnick, S.; Ngo, T.; Nguyen, D. T.; Prodhom, B.; Reiher, W. E., III; Roux, B.; Schlenkrich, M.; Smith, J.; Stote, R.; Straub, J.; Watanabe, M.; Wiork-iewicz-Kuczera, J.; Yin, D.; Karplus, M. *J. Phys. Chem. B* **1998**, *102*, 3586−3616.
(17) Feig, M.; MacKerell, A. D.; Brooks, C. L., III. *J. Phys. Chem. B* **2003**, *107*, 2831−2836.
(18) MacKerell, A. D.; Feig, M.; Brooks, C. L., III. *J. Am. Chem. Soc.* **2004**, *126*, 698−699.
(19) MacKerell, A. D.; Feig, M.; Brooks, C. L., III. *J. Comput. Chem.* **2004**, in press.
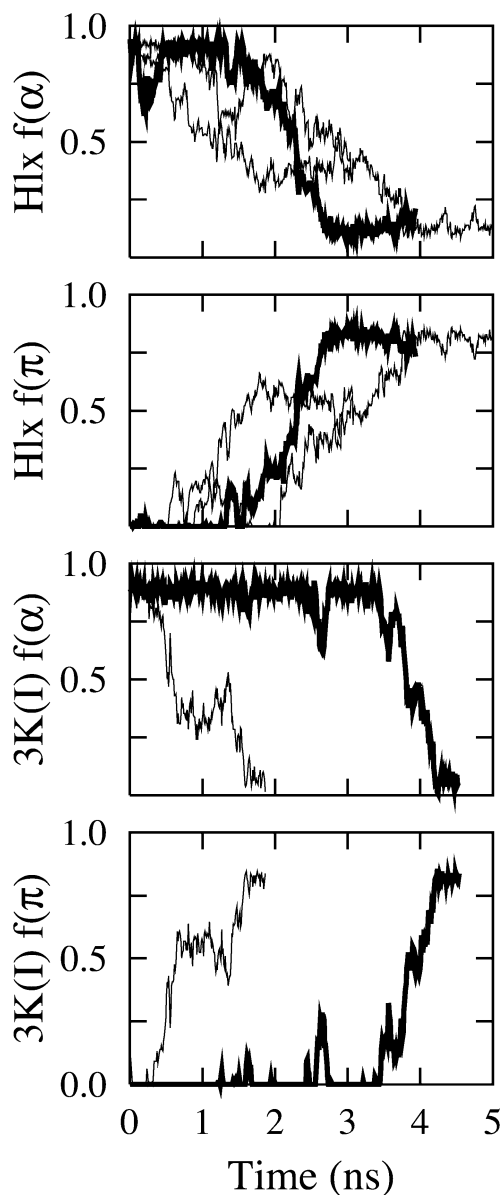
Figure 1. Fraction of α- and π-helix in simulations of Ac-WAAAH-(AAARA)₃A-NH₂ (*Hlx*) and Ac-(AAAAK)₃A-NH₂ (3K(I)) using the parameter set C22 at 293 K with 1 M NaCl (light lines) and neutralizing ions only (dark lines).

to date has not included simulations in explicit solvent of peptides of sufficient length to form α- or π-helices.

We next consider a less obvious question: Might *Hlx* indeed contain a significant fraction of π-helix? This is addressed because the α-helicity of *Hlx* was established by circular dichroism (CD).[13] While CD is a well-established tool for structure analysis in proteins and peptides,[20] caution must be applied when ruling out conformations using this method. Recently, for example, two β-peptides, one folded and the other unfolded, were shown to have the same CD spectra.[21] A variety of considerations suggest that it would be difficult to exclude the presence of π-helix for a short peptide in solution from CD alone. The ideal ϕ,ψ values are ($-57°$, $-47°$) and ($-57°$, $-70°$) for α- and π-helices, respectively;[1,22] i.e., the π-helix is slightly

more open as would be expected from its hydrogen-bonding pattern. Manning and Woody[23] used these dihedral angle values to predict CD spectra. While the maximum and two minima of each spectrum are at similar wavelengths, the higher wavelength minimum of the π-helix is predicted to be more shallow and broad, suggesting that these helices are distinguishable by CD. However, recent analyses[24,25] of high-resolution protein crystal structures have identified a greater than expected number of π-helices, and these do not conform to the ideal values: the observed average ϕ,ψ values are ($-76°$, $-41°$) with standard deviations of 25° and 24°, respectively. Likewise, the average ϕ,ψ of α-helices in proteins are ($-62°$, $-41°$), with standard deviations of 7°.[26] Hence, there is considerable overlap with the backbone dihedrals of α- and π-helices. Experimental and calculated CD spectra of α-helical peptides also show substantial dependence on both length and composition,[21,27−30] further complicating any comparison. NMR measurements indicate significant populations of 3₁₀-helices in 3K(I),[31] opening the possibility of other helical forms for *Hlx*. Last, perhaps because π-helical stretches in proteins are typically only two turns and seldom more than four,[25] we are not aware of any experimental CD results on such helices.

Measurement of NOEs by NMR is also an important tool for determining protein structure,[32] and it is reasonable to assume that it may be applied to deduce the absence of significant π-helix in a peptide. However, the considerable variation in backbone angles in α- and π-helices, their dynamic fluctuations, and the possibility of bifurcated hydrogen bonds make an NOE-based approach cumbersome and potentially uncertain.

By far the most direct way to distinguish the helices is to probe their hydrogen-bonding patterns. This can be accomplished using the HNCO experiment. This NMR technique was originally designed by Bax and co-workers[33,34] to correlate the HN of an amino acid residue and the carbonyl carbon of the preceding residue of a fully $^{13}C-^{15}N$ labeled protein (Figure 2, relevant atoms boxed in thin sold lines). More recently, Grzesiek and co-workers[35,36] detected inter-residue hydrogen bonds in ubiquitin and an S-peptide analogue using the same pulse sequence with delays adjusted to suppress magnetization transfer between adjacent residues (Figure 2, bold lines). Here the HNCO method is applied to three selectively labeled ^{15}N and ^{13}C isotopologs (isotopic homologues)[37] of *Hlx* to probe for hydrogen bonds between residues 8 and 11 (characteristic of a

(20) *Circular Dichroism: Principles and Applications*; Berova, N., Nakanishi, K., Woody, R. W., Eds.; Wiley-VCH: New York, 2000.
(21) Glattli, A.; Daura, X.; Seebach, D.; van Gunsteren, W. F. *J. Am. Chem. Soc.* **2002**, *124*, 12972−12978.
(22) Ramachanrdan, G. N.; Sasisekharan, V. *Adv. Protein Chem.* **1968**, *23*, 283−438.
(23) Manning, M. C.; Woody, R. *Biopolymers* **1991**, *31*, 569−586.
(24) Weaver, T. M. *Protein Sci.* **2000**, *9*, 201−206.
(25) Fodje, M. N.; Al-Karadahhi, S. *Protein Eng.* **2002**, *15*, 353−358.
(26) Barlow, D. J.; Thornton, J. M. *J. Mol. Biol.* **1988**, *201*, 601−619.
(27) Chakrabartty, A.; Kortemme, T.; Padmanabhan, S.; Baldwin, R. L. *Biochemistry* **1993**, *32*, 5560−5565.
(28) Chin, D. H.; Woody, R. W.; Rohl, C. A.; Baldwin, R. L. *Proc. Natl. Acad. Sci. U.S.A.* **2002**, *99*, 15416−15421.
(29) Gans, P. J.; Pingchiang, C. L.; Manning, M. C.; Woody, R. W.; Kallenbach, N. R. *Biopolymers* **1991**, *31*, 1605−1614.
(30) Hirst, J. D.; Brooks, C. L., III. *J. Mol. Biol.* **1994**, *243*, 173−178.
(31) Millhauser, G. L.; Stetland, C. J.; Hanson, P.; Bolin, K. A.; van de Ven, F. J. M. *J. Mol. Biol.* **1997**, *267*, 963−974.
(32) Cavanagh, J.; Fairbrother, W. J.; Palmer, A. G.; Skelton, N. J. *Protein NMR Spectroscopy, Principles and Practice*, 1st ed.; Academic Press: San Diego, CA, 1996.
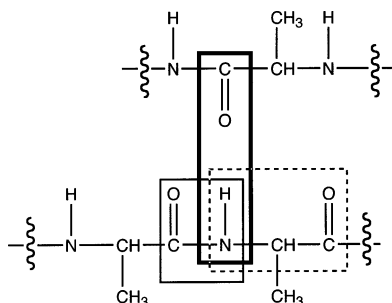(33) Kay, L. E.; Ikura, M.; Tschudin, R.; Bax, A. *J. Magn. Reson.* **1990**, *89*, 496−514.
(34) Grzesiek, S.; Bax, A. *J Magn. Reson.* **1992**, *96*, 432−440.
(35) Cordier, F.; Grzesiek, S. *J. Am. Chem. Soc.* **1999**, *121*, 1601−1602.
(36) Jaravine, V. A.; Alexandrescu, A. T.; Grzesiek, S. *Protein Sci.* **2001**, *10*, 943−950.
(37) Seeman, J. I.; Secor, H. V.; Disselkamp, R.; Bernstein, E. R. *J. Chem. Soc., Chem. Commun.* **1992**, *9*, 713−714.

Figure 2. Three paths for magnetization transfer in the HNCO experiment: between adjacent residues (rectangle with thin solid lines); between hydrogen-bonded residues (bold lines); and intraresidue (dashed lines). In each case the path of magnetization transfer is from H → N → C(O) → N → H.

3_{10}-helix), 8 and 12 (α-helix), and 8 and 13 (π-helix). Presence of a correlation peak in the HNCO spectrum of one isotopolog and absence in the other two allows identification of the dominant helical form.

A third question was motivated by the observation that the signal-to-noise ratio of the peptide HNCO measurement is approximately one-tenth of that observed for ubiquitin under equivalent conditions. This is not unexpected: kinetic data indicate that *Hlx* unfolds and refolds on the microsecond time scale,[38] while the HNCO measurements as devised require 300 ms for the necessary coherence transfers. It is also possible that the hydrogen bonds of the peptide, when formed, are qualitatively weaker than those of ubiquitin. MD simulations of ubiquitin were carried out and compared with those of *Hlx* to evaluate the relative strength of their hydrogen bonds.

Materials and Methods

Molecular Dynamics Simulations. The CHARMM program[15] was used for model building, energy minimization, MD simulations, and analyses of simulation data, with a few exceptions noted below. Standard CHARMM C22 protein parameters,[16] including the modified TIP3P water model,[39] were used. These protein parameters were augmented with two different versions of the CMAP grid corrections: an initial "emp9i" preliminary version[18] and the more recent "emp16j",[19] here denoted C22/CMAP. The energy minimization protocol started with a small (10−50) number of steps with a simple steepest descent algorithm, followed by more extensive (100−500 steps) minimization with an adopted-basis Newton−Raphson algorithm.

For the simulations of *Hlx* and 3K(I), the peptide was inserted into a pre-equilibrated 59.0 Å/edge cubic box of water; waters within 2.6 Å of any solute atom were deleted. To achieve an electrically neutral system (desirable for Ewald summation), four or three chloride ions, for *Hlx* and 3K(I), respectively, were added by replacing randomly selected water molecules that were more than 6 Å from any solute atom. For simulations denoted 1 M salt, 134 sodium ions and 134 chloride ions were added, again via replacement of randomly selected water molecules; candidates for replacement were required to be more than 6 Å from any solute atom or previously placed ion. The final systems were energy-minimized with periodic boundary conditions applied; multiple models (five or 10) were built, and the one with lowest energy after minimization was chosen for the simulation. For these minimizations and the MD simulations, the Lennard-Jones potential was switched to zero over the interval from 7 to 10 Å; the electrostatic potential was evaluated with particle mesh Ewald summation, with a

fifth-order spline interpolation for the complementary error function, $\kappa = 0.34$ Å^{-1}, a real space cutoff of 10 Å, and 64 grid points (i.e., spacing for the mesh was just under 1 Å), and dielectric constant $\epsilon = 1.0$. The systems were then equilibrated at constant pressure by heating from 93 to 293 K over the first 4 ps and stabilizing for 96 ps, using velocity reassignment and the Langevin Piston with pressure piston mass and collision frequency of 2000 amu and 25 ps^{-1}, respectively. Damping on the pressure piston was removed, and constant pressure and temperature simulations were then carried out with a thermal piston mass of 20 000 kcal/ps^2. Each system was simulated for up to 5 ns, including the initial 100 ps of equilibration, with coordinate sets saved every picosecond for later analyses. The time step for all MD simulations equaled 0.001 ps.

Simulations of the protein ubiquitin were based on the NMR structure *model 1* from PDB[40] entry 1D3Z.[41] The protein heavy atom coordinates were imported, hydrogens were placed, and the protein coordinates were then energy-minimized with the backbone restrained. The protein was solvated by insertion into a rhombic dodecahedron with 60 Å between opposing parallel faces, followed by deletion of water molecules within 2.5 Å of any protein atom. (The rhombic dodecahedron was prepared from a sphere of water molecules with the same volume; the polyhedral periodic boundary was imposed, and the pure water system was equilibrated via 150 ps of MD.) The solvated protein was energy-minimized, with the protein initially fixed with rigid constraints; the constraints were removed, and more extensive minimization was performed. Forty chloride and 40 sodium ions were added via randomly selected water replacement, as for the peptide systems; 100 ion configurations were generated and energy-minimized, and the lowest energy configuration was saved. The system was heated from 198 to 298 K over 10 ps, equilibrated for another 40 ps at 298 K, and then kept at 298 K with a thermostat, as above. The Ewald mesh was 60 grid points in each dimension, keeping the spacing close to 1 Å. The remaining details are as for the helical simulations.

Hydrogen bond patterns were evaluated by first processing the stored MD simulation trajectories and, for each stored coordinate set, extracting H-bond pair lists with a CHARMM H-bond energy of less than −0.5 kcal for backbone N−H and C=O groups. A Fortran program was used to process these pair lists by counting pairs that matched the intervals $i, i + 3$, $i, i + 4$, and $i, i + 5$ corresponding to the 3_{10}-, α-, and π-helix types, respectively. The counts were converted to a fraction by dividing by N-3 for an N residue helix, which was the maximum number of H-bonds observed for both *Hlx* and 3K(I) simulations and is one more than the ideal α-helix. The five central $i, i + 4$ H-bonds for *Hlx* and the primary ubiquitin α-helical region (residues 22−35) were examined in more detail as time series of H-bond distance (H to O) and CHARMM H-bond energy.

Peptide Synthesis and Characterization. Unlabeled Ac-WAAAH-(AAARA)$_3$-A-NH$_2$ and three isotopologs (isotopic homologues)[37] were prepared by solid-phase synthesis. For the latter, FMOC-protected ^{13}C, ^{15}N doubly labeled alanines were incorporated at two residues in each peptide: A8 and A11 (*Hlx$_{8-11}$*), A8 and A12 (*Hlx$_{8-12}$*), and A8 and A13 (*Hlx$_{8-13}$*). The peptides were purified using reversed-phase HPLC, and their masses were confirmed via an ABI voyager matrix-assisted laser desorption time-of-flight (MALDI-TOF) mass spectrometer. CD spectra were recorded at 278 K, with a peptide concentration of 100 μM in 20 mM sodium d_3-acetate buffer, pH 4.9 in a cell with a path length of 0.01 cm. Spectra of the unlabeled peptide agree with previously reported results.[13]

NMR. Samples were prepared by dissolving ca. 2.5 mg of *Hlx* in 230 μL, 20 mM sodium d_3-acetate at pH 4.9. The buffer was made with 90% H$_2$O and 10% D$_2$O for locking purposes. The resulting

(38) Thompson, P. A.; Munoz, V.; Jas, G. S.; Henry, E. R.; Eaton, W. A.; Hofrichter, J. *J. Phys. Chem. B* **2000**, *104*, 378−389.
(39) Durell, S. R.; Brooks, B. R.; Ben-Naim, A. *J. Phys. Chem.* **1994**, *98*, 2198−2202.

(40) Berman, H. M.; Westbrook, J.; Feng, Z.; Gilliland, G.; Bhat, T. N.; Weissig, H.; Shindyalov, I. N.; Bourne, P. E. *Nucleic Acids Res.* **2000**, *28*, 235−242.
(41) Cornilescu, G.; Marquardt, J. L.; Ottinger, M.; Bax, A. *J. Am. Chem. Soc.* **1998**, *120*, 6836.

samples were placed in Shigemi (Allison Park, PA) microcells. NMR experiments were performed at 278 K (where helix content is approximately 80%)[13] on a Bruker Avance spectrometer operating at 800 MHz ^{1}H frequency using a triple resonance probe equipped with shielded *x,y,z* gradients. (The molecular dynamics simulations were carried out at a higher temperature, 293 K, for enhanced conformational sampling.)

One-dimensional ^{13}C spectra were taken with the carrier frequency at 100 ppm, a spectral window of 200.4 ppm, 32 768 data points, and a relaxation delay of 1.25 s. Multidimensional experiments were measured using carefully optimized WATERGATE and flip-back methods for effective water suppression.[42,43] Carrier frequencies were set to H$_2$O (4.96 ppm at 278 K) in ^{1}H, 120 ppm in ^{15}N, and 180 ppm in ^{13}C. In each conventional (non-TROSY) HSQC experiment, ^{1}H and ^{15}N spectral windows were set to 13.9 ppm (1024 complex points) and 32 ppm (256 complex points), respectively. Four scans per t_1 point were accumulated for the HSQC experiments (henceforth the modifier *per t_1 point* is assumed). Each data set was zero filled to 2048 total points in ^{1}H and 512 total points in ^{15}N. The TROSY version of Cordier and Grzesiek's HNCO experiment[35,44,45] was performed on each of the three labeled peptides to probe for a hydrogen bond *between the labeled residues*. In each HNCO experiment, ^{1}H and ^{13}C spectral windows were set to 13.95 ppm (2048 complex points) and 3 ppm (40 complex points), respectively. The total time needed for the coherence transfer in the HNCO was approximately 300 ms.

For *Hlx$_{8-12}$*, four blocks of 128 scans and one block of 512 scans were summed and then processed. For *Hlx$_{8-11}$* and *Hlx$_{8-13}$*, 12 blocks of 128 scans were measured with receiver gain doubled. Spectra of *Hlx$_{8-11}$* and *Hlx$_{8-13}$* presented in the next section show the HNCO spectra corresponding to 1024 scans, though a total of 1536 scans were also summed for analysis. The 1024- and 1536-scan experiments required 30 and 45 h, respectively.
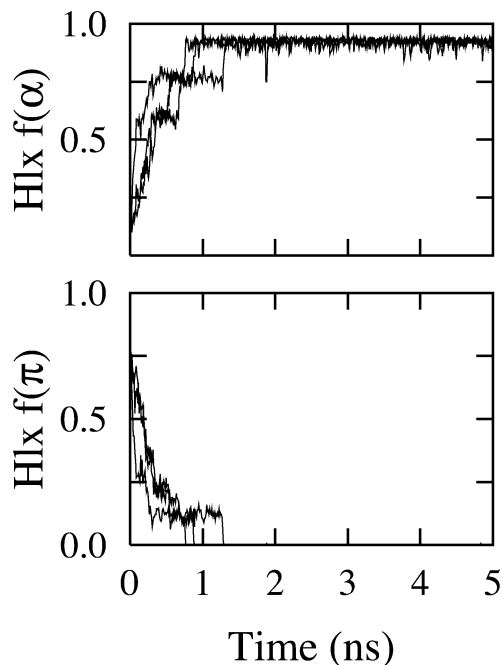
Spectra of ubiquitin were measured under similar conditions to those reported by Cordier and Grzesiek.[35] Spectral windows in ^{1}H and ^{13}C were set to 13.95 ppm (2048 complex points) and 14 ppm (130 complex points), respectively. Each t_1 point was the result of 128 scans, the ^{1}H carrier was set to the H$_2$O frequency, and the ^{13}C carrier was set to 177 ppm.

Data were processed using nmrPipe and displayed with nmrDraw.[46] PIPP was used to generate figures displaying NMR spectra.[47]

Results

Molecular Dynamics Simulations. Figure 3 displays the essential simulation result of this article: in three replicate 5-ns simulations of *Hlx* in 1 M NaCl using C22/CMAP, the all-π-helical initial condition converted to approximately 90% α-helix in about 1 ns, leaving no discernible π-helix. Similar results were obtained in simulations of *Hlx* and 3K(I) using the preliminary version of C22/CMAP[18] at 293 K (Figure 4) and 273 K (data not shown). Hence, C22/CMAP strongly favors α- over π-helices in water.

Determination of Hydrogen Bonds by HNCO. Table 1 lists the relevant ^{13}C, ^{1}H, and ^{15}N chemical shifts for each peptide. One-dimensional ^{13}C spectra for the isotopologs of *Hlx* show two doublets in the carbonyl region, each due to coupling of the carbonyl carbon to a neighboring ^{13}C$_\alpha$ atom. These doublets

(42) Piotto, M.; Saudek, V.; Sklenar, V. *J. Biomol. NMR* **1992**, *2*, 661−665.
(43) Grzesiek, S.; Bax, A. *J. Am. Chem. Soc.* **1993**, *115*, 12593−12594.
(44) Wang, Y. X.; Jacob, J.; Cordier, F.; Wingfield, P.; Stahl, S. J.; Lee-Huang, S.; Torchia, D.; Grzesiek, S.; Bax, A. *J. Biomol. NMR* **1999**, *14*, 181−184.
(45) Loria, J. P.; Rance, M.; Palmer, A. *J. Magn. Reson.* **1999**, *141*, 180−184.
(46) Delaglio, F.; Grzesiek, S.; Vuister, G.; Zhu, G.; Pfeifer, J.; Bax, A. *J. Biomol. NMR* **1995**, *6*, 277−293.
(47) Garrett, D. S.; Powers, R.; Gronenborn, A. M.; Clore, G. M. *J. Magn. Reson.* **1991**, *95*, 214−220.

Figure 3. Fraction of α- and π-helix in three simulations of *Hlx* in 1 M NaCl using the parameter set C22/CMAP. There was no π-helix after 1.2 ns.
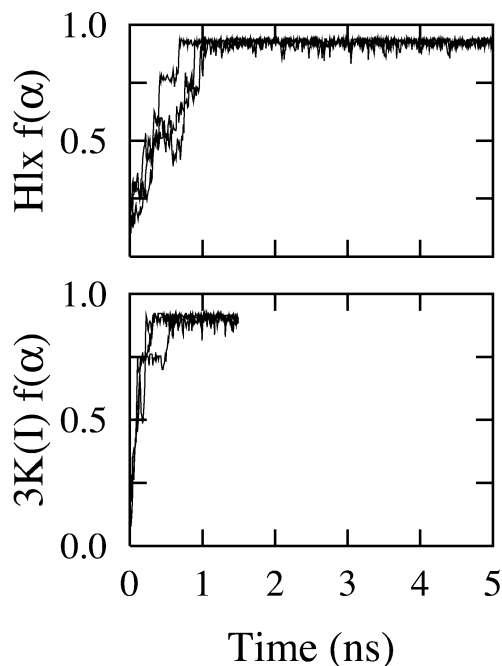
Figure 4. Fraction of α-helix in three simulations of *Hlx* and 3K(I) in 1 M NaCl using the preliminary version[18] of C22/CMAP. The simulations of 3K(I) were terminated at 1.5 ns.

also served to confirm isotopic incorporation. Assignment of A8, A11, A12, and A13 was straightforward when all three ^{1}H−^{15}N HSQC spectra were compared. Since A8 is isotopically labeled in each peptide, its chemical shifts are expected to remain the same. In each peptide one additional residue is labeled. ^{1}H and ^{15}N assignments were made by elimination. Similar logic was used to assign the ^{13}C peaks for the peptides. ^{13}C chemical shifts were calculated as the midpoint between each doublet.

The assignments listed in Table 1 predict that a hydrogen bond between C=O of A8 and HN of A11 would be indicated

Table 1. [1]H, ^{15}N, and [13]C Chemical Shifts of Relevant Alanine Residues in the *Hlx* Isotopologs

residue	[1]H ppm[a]	[15]N ppm[a]	[13]C ppm[b]
Ala 8	8.01 ± 0.01	123.54 ± 0.06	180.88 ± 0.01
Ala 11	8.11 ± 0.01	122.68 ± 0.06	180.56 ± 0.01
Ala 12	8.05 ± 0.01	122.54 ± 0.06	180.41 ± 0.01
Ala 13	8.01 ± 0.01	123.54 ± 0.06	180.70 ± 0.01

[a] From two-dimensional [1]H−^{15}N HSQC spectra, corrected for TROSY spectrum by −0.065 ppm in ^{1}H and −0.67 ppm in [15]N. [b] From one-dimensional ^{13}C spectra.

by a correlation peak at 8.11 ± 0.01 (the ^{1}H shift of A11), 180.88 ± 0.01 ppm (the ^{13}C chemical shift of A8) in the HNCO spectrum of Hlx_{8-11}. Similarly, an H-bond between A8 and A12 is indicated by a peak at 8.05 ± 0.01, 180.88 ± 0.01 ppm in the spectrum of Hlx_{8-12}; and one between A8 and A13 by a peak at 8.01 ± 0.01, 180.88 ± 0.01 ppm in the spectrum of Hlx_{8-13}. Note that the chemical shifts of ^{13}C are the same (the acceptor is always A8), while those of ^{1}H vary (the donors are different).

Figure 5 presents the HNCO spectra for the three peptides. Hlx_{8-12} (middle panel) shows clear evidence of a hydrogen bond: a correlation peak at 8.06 ± 0.01, 180.86 ± 0.8 ppm, with a signal-to-noise (S/N) ratio of more than 10:1. In contrast, HNCO spectra for peptides Hlx_{8-11} and Hlx_{8-13} (top and bottom, respectively) do not show correlation peaks at the chemical shifts noted in the preceding paragraph, even when the total number of scans was increased from 1024 to 1536 (data not shown). The data demonstrate that *Hlx* forms an α-helix.

Comparison with Ubiquitin. In previously published studies[35] and here (data not shown), 128 scans were sufficient to obtain strong HNCO peaks for residues in the center of the principal α-helix in ubiquitin; i.e., 8 times fewer than required for Hlx_{8-12} under otherwise similar conditions.

One possible explanation for this difference is based on the previously published observation of transitions between folded and unfolded states of *Hlx*.[38] In the present HNCO experiment, coherence is transferred from the amide proton to its attached nitrogen, to the hydrogen-bonded carbonyl carbon, and back again on a time scale of about 300 ms. The chemical shifts for the folded peptide differ from those in the unfolded peptide. Chemical shifts change with each folding−unfolding event, and the various coherences in the HNCO experiment are slightly dephased provided the exchange is not too rapid. The cumulative dephasing during the approximately 300 ms of the HNCO coherence transfer would be expected to lead to signal loss.

It is also possible that the hydrogen bonds in the peptide are distorted, thereby lowering the apparent coupling constant $^{3h}J_{NC'}$ and the intensity of the signal. To test whether the hydrogen bonds in the folded peptide are comparable to a folded protein, 5-ns simulations of ubiquitin were carried out with both C22/CMAP and C22. The average hydrogen bond lengths and energies and their fluctuations of five residues in the indicated α-helix of ubiquitin were then compared with the central five residues of *Hlx*. As shown in Table 2, there are no significant differences in the behavior of the hydrogen bonds between the protein and the peptide on the 5-ns time scale. Hence, peptide unfolding and refolding is responsible for the low sensitivity of the peptide HNCO measurement on Hlx_{8-12}.

Note also that the averages for C22/CMAP and C22 are statistically indistinguishable for ubiquitin. One may infer that
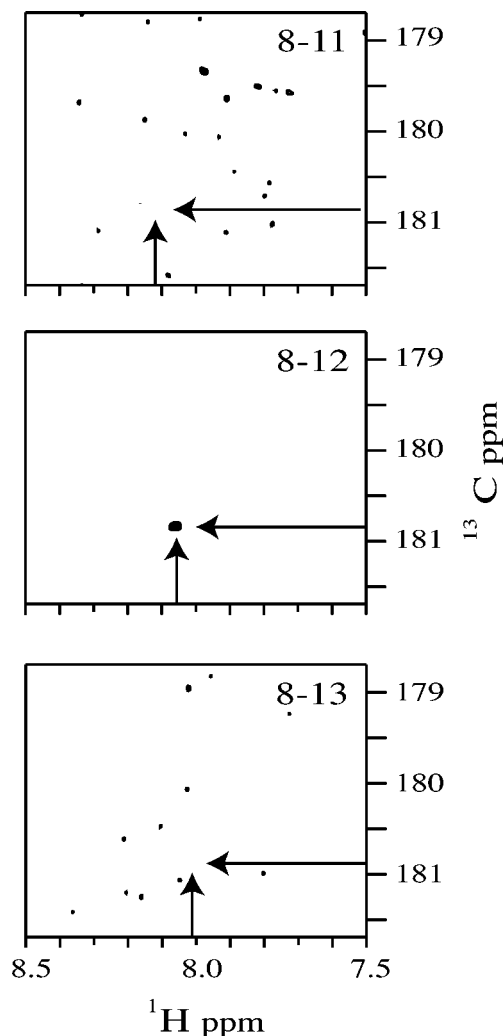
Figure 5. HNCO-TROSY spectra of Hlx_{8-11} (top), Hlx_{8-12} (middle), and Hlx_{8-13} (bottom), with the positions of the predicted correlation peaks for each helical form denoted with arrows. A correlation peak for Hlx_{8-12} is evident at 8.06 ± 0.01 ppm in ^{1}H and 180.86 ± 0.08 ppm in ^{13}C, indicating a hydrogen bond between residues 8 and 12; i.e., an α-helix. Corresponding correlation peaks for Hlx_{8-11} and Hlx_{8-13} are below the limit of detection. The spectra for Hlx_{8-11} and Hlx_{8-13} were acquired with a receiver gain set twice as high as that for Hlx_{8-12}, and consequently they are noisier.

the protein scaffolding helps maintain the α-helical structure, and thus the deficiency in C22 only becomes apparent when simulating peptides in solution for a sufficiently long time.

Discussion and Conclusions

We have established by molecular dynamics simulation that the potential C22/CMAP strongly favors α-helical over π-helical conformations for two short peptides, *Hlx* and 3K(I), in solution. HNCO NMR measurements probing for hydrogen bonds between residues 8−11, 8−12, and 8−13 of *Hlx* confirm that this region is indeed α-helical, as consistent with the original CD measurements.[13,14] There is no evidence of either 3₁₀- or π-helix from NMR at the preceding residues.

It has been assumed that the $^{3h}J_{NC'}$ couplings for the hydrogen bond in each helical type are comparable. HNCO cross-peaks in proteins have been observed for hydrogen bonds in β-sheets and β-turns in addition to α-helices, with values of $^{3h}J_{NC'}$ ranging from −0.1 to −0.85 Hz.[48,49] Recently, $^{3h}J_{NC'}$ values of 0.07−0.11 were observed for 3₁₀-helices of penta- and hexapeptides

Table 2. Average Lengths (Å), Energies (kcal/mol), and Energy Fluctuations (kcal/mol) of Hydrogen Bonds for *Hlx* and Ubiquitin from the Final 3 ns of Each Trajectory[a]

Hlx	CMAP			Ubi	CMAP			C22		
res	$\langle r \rangle$	$\langle E \rangle$	$\langle \delta E^2 \rangle^{0.5}$	res	$\langle r \rangle$	$\langle E \rangle$	$\langle \delta E^2 \rangle^{0.5}$	$\langle r \rangle$	$\langle E \rangle$	$\langle \delta E^2 \rangle^{0.5}$
10	2.11	−2.60	0.91	26	2.21	−2.51	0.86	2.24	−2.49	0.95
11	2.09	−2.65	0.87	27	2.09	−3.16	0.78	2.02	−3.44	0.77
12	2.11	−2.60	0.87	28	2.13	−2.39	0.92	2.16	−2.28	1.01
13	2.14	−2.43	0.91	29	2.18	−2.40	0.98	2.23	−2.25	1.09
14	2.11	−2.81	0.93	30	2.21	−2.77	0.86	2.21	−2.69	0.94
ave	2.11	−2.62	0.90		2.16	−2.65	0.88	2.17	−2.63	0.95
SD	0.02	0.14	0.01		0.05	0.33	0.08	0.09	0.49	0.12

[a] In each case the residue number, *res*, indicates the position of the donor NH group (the acceptor CO group is on *res−4*). C22 results are only included for ubiquitin, because the α-helical form of *Hlx* is not stable with this parameter set.

modified for increased rigidity.[50] To our knowledge, there is no report of the magnitudes of these couplings for π- or 3_{10}-helices of naturally occurring amino acids. Hypothetically, they could be very small, and π- or 3_{10}-helices would be difficult to detect even when present in substantial fractions. To determine whether this is likely, it is reasonable to begin with the empirical relation determined by Cornilescu et al.:[49] $^{3h}J_{NC'} = -59\,000\exp(-4R_{NO}) \pm 0.09$ Hz, where R_{NO} is the distance between the donor nitrogen and acceptor oxygen. From the preceding equation, $R_{NO} = 3.3$ Å yields $|^{3h}J_{NC'}| = 0.1$ Hz. If R_{NO} were larger than 3.3 Å in π- or 3_{10}-helices in proteins, then these helices would indeed be difficult to discern. Examples of π-helical regions in crystal structures of proteins were obtained from Table 1 of ref 25. On the basis of 66 distances in 24 structures determined to a resolution of 1.6 Å or less, the average $R_{NO} = 2.94$ Å with a standard deviation of 0.15 Å. On this basis, $^{3h}J_{NC'}$ of a π-helix should not differ substantially from that of an α-helix. Likewise, a recent study[51] of protein crystal structures indicates that 3_{10}-helices can form hydrogen bonds comparable to those in α-helices, though instances of $R_{NO} > 3.3$ Å were found in short 3_{10}-helices. While distances less than 3.3 Å do not guarantee a substantial coupling constant (other distortions can lower the magnitude), it is likely that π- or 3_{10}-helices would have been observed if they were present.

Both the simulation and NMR results mostly pertain to the center of the helix; i.e., neither provide direct insight into the behavior of the termini. Only hydrogen bonds associated with residue 8 were probed in the experiment, and the simulations may not have been run sufficiently long to explore the full range of conformations at the termini. It is possible that other helical forms, such as the 3_{10}, could be present near the ends. However, the N-terminus of *Hlx* was designed[13] to fold into an α-helix by taking advantage of the favorable stacking of Trp1 and His5. Hence, it is unlikely that a π-helix is present if it is unfavored at the N-terminus, explicitly excluded in the center by NMR (Figure 5, bottom), and shown to be unstable in simulations with C22/CMAP.

Small folded peptides are in equilibrium with unfolded states,[36,38,52,53] and *Hlx* is no exception: the helical content is

80% at 278 K (the temperature of the HNCO experiment) and 60% at 293 K (the temperature of the MD simulation).[13] The present simulations do not speak to this equilibrium because unfolding and refolding is on the microsecond time scale or longer, well out of the present range of MD simulations in explicit solvent (though progress is being made[54,55]). Hence, the 90% helical content shown in Figures 3 and 4 represents only the folded state. Uncertainty in this value arises from the precise assignment of a helix (definitions based on dihedral angle or energy cutoffs vary) and isomerizations (i.e., fraying) at the ends. These simulations also indicate that the hydrogen bonds in the center of the folded peptide are as stable as those in ubiquitin on very short time scales (Table 2). Kinetic modeling by Thompson et al.[38] suggests that *Hlx* is almost entirely helical when folded, in agreement with the simulation results herein.

The HNCO measurements can provide insight into the equilibrium between folded peptide and random coil.[36] The intensity of the overall NMR signal is a population-weighted average of the signals for the helix and unfolded states. No correlation is expected for the unfolded state because hydrogen bonds are not fully formed.[36,49] Consequently, the intensity of the correlation peak can be reduced at higher temperatures as a result of changes in equilibrium populations. Future studies will consider the kinetic and thermodynamic nature of the equilibrium in *Hlx*.

As a final technical point regarding the HNCO measurement, an intraresidue transfer is also possible when both the nitrogen and carbon are labeled (Figure 2, dashed lines). Although the value of the intraresidue $^2J_{NC'}$ coupling is estimated to be on the same order of magnitude as the $^{3h}J_{NC'}$ couplings across the hydrogen bonds,[35,56] no intraresidue correlations were observed for any of the peptides under study (Figure 5). This suggests that motion associated with folding and unfolding substantially reduces $^2J_{NC'}$, or that it is smaller than previously thought.

The CMAP approach developed by Feig, MacKerell, and Brooks[17−19] represents a significant technical advance in the treatment of potential energy functions for strongly coupled dihedral angles such as those in peptide linkages. A key feature of these linkages is that their potential energy surfaces are not easily modeled by sums of independent periodic functions. This helps explain why π-helical conformations in peptides have been so readily generated in simulations: the α- and π-motifs are close together on the ϕ,ψ surface, and it is difficult to fine-tune the standard potential energy functions to allow one and to

(48) Grzesiek, S.; Cordier, F.; Dingley, A. J. In *Methods in Enzymology*; James, T. L., Dötsch, V., Schmitz, U., Eds.; Academic Press: San Diego, CA, 2001; Vol. 338, Part A, pp 111−133.
(49) Cornilescu, G.; Ramirez, B. E.; Frank, K. K.; Clore, G. M.; Gronenborn, A. M.; Bax, A. *J. Am. Chem. Soc.* **1999**, *121*, 6275−6279.
(50) Bellanda, M.; Rainaldi, M.; Broxterman, Q. B.; Kaptein, B.; Formaggio, F.; Crisma, M.; Toniolo, C. *Angew. Chem., Int. Ed.* **2004**, *43*, 3152−3155.
(51) Pal, L.; Chakrabarti, P.; Basu, G. *J. Mol. Biol.* **2003**, *326*, 273−291.
(52) Huang, C.-Y.; Getahun, Z.; Wang, T.; DeGrado, W. F.; Gai, F. *J. Am. Chem. Soc.* **2001**, *123*, 12111−12112.
(53) Werner, J. H.; Dyer, R. B.; Fesinmeyer, R. M.; Andersen, N. H. *J. Phys. Chem. B* **2002**, *106*, 487−494.

(54) Brooks, C. L. *Curr. Opin. Struct. Biol.* **1998**, *8*, 222−226.
(55) Daggett, V. *Acc. Chem. Res.* **2002**, *35*, 422−429.
(56) Sattler, M.; Schleucher, J.; Griesinger, C. *Prog. Nucl. Magn. Reson. Spectrosc.* **1999**, *34*, 93−158.

exclude the other. This complexity contrasts with alkanes, where the positions of individual minima are well-separated and largely independent of chain length. Hence, alkanes are well-modeled with a combination of independent torsional terms and non-bonded interactions.[57] CMAP, or grid-corrected, potentials will be useful for the parametrization of other highly coupled torsion pairs, such as glycosidic linkages in polysaccharides.

Likewise, building on previous work,[33−36] it has been demonstrated that hydrogen bonds in small peptides in aqueous solution can be directly detected by NMR. Particularly important is that sufficient signal is observed even though the peptide likely unfolds and refolds many times over the course of the measurement. Hence, the HNCO method can be used to probe peptide

and protein secondary structure even when folding and unfolding are present.

(57) Feller, S. E.; MacKerell, A. D. *J. Phys. Chem. B* **2000**, *104*, 7510−7515.